

TECHNICAL NOTE: SIMULATION OF AN H₂/O₂ FLAME BY THE LEAST-SQUARES FINITE ELEMENT METHOD

SHENG-TAO YU

NYMA SETAR Team, NASA Lewis Research Center, Brook Park, OH, U.S.A.

BO-NAN JIANG

Institute for Computational Mechanics and Propulsion, OAI, NASA Lewis Research Center, Cleveland, OH, U.S.A.

NAN-SUEY LIU

NASA Lewis Research Center, Cleveland, OH, U.S.A.

AND

JIE WU

Institute for Computational Mechanics and Propulsion, OAI, NASA Lewis Research Center, Cleveland, OH, U.S.A.

SUMMARY

The aim of this paper is to use the least-squares finite element method to simulate a quasi-one-dimensional H₂/O₂ flame with comprehensive physical property models.

KEY WORDS LSFEM; reacting flows

1. INTRODUCTION

Recent developments in computational fluid dynamics yielding faster and more robust flow solvers have kindled the pursuit of calculations with detailed chemical kinetics. In this work we employ the least-squares finite element method (LSFEM)¹ to simulate a quasi-one-dimensional flame with comprehensive physical property models. This work is a building block for applying the LSFEM to simulate chemically reacting flows. In parallel, we have used the LSFEM for solving low-Mach-number compressible flows^{2,3} which are complementary to the present work.

Quasi-one-dimensional, premixed, flat flames are commonly used to study flame structure and reaction kinetics. In the past, owing to their simple geometry and wide applications, many flat flames were thoroughly studied both experimentally and numerically. To simulate an H₂/O₂ flat flame, we employ a finite rate kinetics model with eight species and 18 reaction steps. Detailed transport and thermodynamic models for each species and gas mixture are included. In spite of the computational effort, it is plausible to employ comprehensive physical property models; simplified models usually result in inferior predictions. In the calculation we first discretize the time-marching term according to the first-order backward difference. By introducing new variables, the transport equations are then cast into a set of first-order equations. Based on these first-order equations, the least-squares functional is constructed and minimized to obtain the solution. For each new time step the transport properties and finite rate reaction mechanism are updated accordingly. The calculation continues until convergence.

In the next section the governing equations and physical property models are presented. In Section 3 we illustrate the LSFEM for the multiple-species system. In Section 4 we present the simulated results and their comparison with the experimental data of Eberius *et al.*⁴

2. THEORETICAL MODEL

As shown in Figure 1, the premixed fuel and oxidizer flow through a porous plate and a flame is stabilized above the burner. The formulation adopted here is similar to that proposed by Hirschfelder *et al.*⁵ Previously, the same formulation was solved by Smooke⁶ using a finite difference method. The flow is assumed to be steady and quasi-one-dimensional. The viscous effect is neglected and the momentum equation is replaced by the assumption of constant pressure. As a result, only the energy and species equations are of concern. For a gas mixture of N_s species the energy equation is

$$\rho a \frac{\partial h}{\partial t} + \dot{m} \frac{\partial h}{\partial x} - \frac{\partial}{\partial x} \left(\frac{\lambda_m a}{C_p} \frac{\partial h}{\partial x} \right) - \frac{\partial}{\partial x} \left(\rho a \sum_{i=1}^{N_s} h_i D_{im} \frac{\partial Y_i}{\partial x} \right) = 0, \quad (1)$$

where ρ is the density, a is the cross-sectional area and h is the enthalpy. Note that the enthalpy is defined by the mass weighting of species enthalpies, such as

$$h = \sum_{i=1}^{N_s} Y_i h_i, \quad (2)$$

where Y_i is the mass fraction of species i . The species enthalpy is given as

$$h_i = h_{i0}^0 + \int_{T_{ref}}^T C_{pi} dT, \quad (3)$$

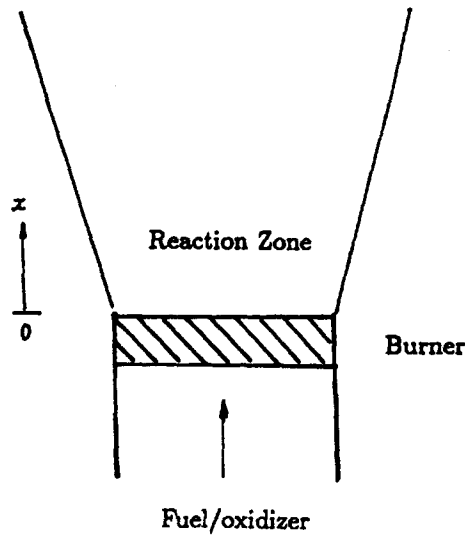


Figure 1. Schematic diagram of premixed hydrogen/oxygen flame

where h_{fi}^0 is the heat of formation at temperature T_{ref} and the integral is the sensible energy. Note that since h_{fi}^0 is included in h , there is no source term in the energy equation. The mass flow rate, i.e. $\dot{m} = \rho ua$, is a prescribed constant. In the heat conduction term, λ_m is the thermal conductivity of the gas mixture. The last term of the energy equation is the heat transfer due to species diffusion and D_{im} is the effective diffusivity of species i in the gas mixture.

The species transport equations considered are

$$\rho a \frac{\partial Y_i}{\partial t} + \dot{m} \frac{\partial Y_i}{\partial x} - \frac{\partial}{\partial x} \left(\rho a D_{im} \frac{\partial Y_i}{\partial x} \right) - \dot{\omega}_i a = 0, \quad i = 1, \dots, N_s, \quad (4)$$

where D_{im} is the effective mass diffusivity of species i in the gas mixture. The source terms $\dot{\omega}_i a$ represents the chemical reactions.

According to the law of mass action,⁷ the stoichiometric equation of a set of N_r elementary reactions involving N_s species is

$$\sum_{i=1}^{N_s} \nu'_{ij} C_i \xrightleftharpoons[K_{bj}]{K_{fj}} \sum_{i=1}^{N_s} \nu''_{ij} C_i, \quad j = 1, \dots, N_r, \quad (5)$$

where C_i is the mole concentration of species i . K_{fj} and K_{bj} are reaction rate constants and are given by the Arrhenius form⁷

$$K_{fj} = A_{fj} T^{B_{fj}} e^{-E_{fj}/RT}, \quad K_{bj} = A_{bj} T^{B_{bj}} e^{-E_{bj}/RT}, \quad (6)$$

where A_f , B_f , A_b , B_b and E_b are given constants associated with the adopted kinetic model and R is the gas constant of the gas mixture. The rate of change of species i by reaction j is

$$(\dot{C}_i)_j = (\nu''_{ij} - \nu'_{ij}) \left(K_{fj} \prod_{i=1}^{N_s} C_i^{\nu'_{ij}} - K_{bj} \prod_{i=1}^{N_s} C_i^{\nu''_{ij}} \right). \quad (7)$$

The total rate of change of species i is

$$\dot{\omega}_i = W_i \sum_{j=1}^{N_r} (\dot{C}_i)_j, \quad (8)$$

where W_i is the molecular weight of species i . In the present paper the species included are H₂, H, OH, H₂O, O, O₂, HO₂ and H₂O₂. To close the system, the equation of state for a gas mixture is imposed:

$$p = \rho R_u T \sum_{i=1}^{N_s} \frac{Y_i}{W_i}. \quad (9)$$

After each numerical iteration, T and ρ of the flow field are calculated by solving the definition of enthalpy, (equations (2) and (3)) and the equation of state (equation (9)).

In modelling the physical properties, C_{pi} is determined by fourth-order polynomials of T :

$$C_{pi} = a_{0i} + a_{1i}T + a_{2i}T^2 + a_{3i}T^3 + a_{4i}T^4. \quad (10)$$

The coefficients are provided by Gordon and McBride.⁸ The specific heat of the gas mixture is obtained by mass concentration weighting: $C_p = \sum_{i=1}^{N_s} Y_i C_{pi}$. The thermal conductivities for each species are least-squares fitted to the following form:

$$\ln \lambda_i = b_{1i} \ln T + \frac{b_{2i}}{T} + \frac{b_{3i}}{T^2} + b_{4i}. \quad (11)$$

Again, the coefficients are provided by Gordon *et al.*⁹ The thermal conductivity of the gas mixture is calculated based on the Wassiljewa equation,¹⁰ which is similar to Sutherland's form for viscosity:

$$\lambda_m = \sum_{i=1}^{N_s} \frac{X_i \lambda_i}{\sum_{j=1}^{N_s} X_j \theta_{ij}}. \quad (12)$$

For species i , X_i is the mole fraction and λ_i is the thermal conductivity. According to Mason and Saxena,¹⁰ the parameter θ_{ij} can be expressed as

$$\theta_{ij} = \kappa \frac{[1 + (\lambda_i/\lambda_j)^{1/2} (M_j/M_i)^{1/4}]^2}{[8(1 + M_i/M_j)]^{1/2}}, \quad (13)$$

where M_i and λ_i are the molecular weight and conductivity of species i respectively and κ is an empirical constant near unity. As used here, $\kappa = 1$.

The binary mass diffusivity D_{ij} between species i and j is obtained using the Chapman–Enskog theory.¹⁰

$$D_{ij} = 0.0188T^{3/2} \frac{[(M_i + M_j)/M_i M_j]^{1/2}}{p \sigma_{ij}^2 \Omega_D}, \quad (14)$$

where p is the pressure and σ_{ij} is the binary Lennard-Jones length in angstroms, which is usually obtained by a simple rule such as $\sigma_{ij} = 0.5(\sigma_i + \sigma_j)$. The Lennard-Jones length of each species, σ_i , is available in Reference 10. Ω_D , the diffusion collision integral, is calculated based on the relation proposed by Neufeld *et al.*¹⁰

In simulating the flow motion of a gas mixture, direct use of binary diffusivity is cumbersome. It is desirable to employ an effective diffusion coefficient D_{im} for each species i in the gas mixture, such as

$$F_i = -D_{im} \frac{\partial Y_i}{\partial x}, \quad (15)$$

where F_i is the diffusion flux and D_{im} can be calculated based on Williams's correlation:⁷

$$D_{im} = \frac{1 - X_i}{\sum_{j \neq i} X_j / D_{ij}}. \quad (16)$$

The adopted property models are rather complex and computationally intensive. However, it was our experience that these complex physical property models are essential for the reactive flow solver to produce satisfactory predictions.

3. LEAST-SQUARES FINITE ELEMENT METHOD

Introducing the heat conduction flux H and the diffusion flux F_i as new variables, the species and energy equations can be reformulated into the form

$$\begin{aligned}\rho a \frac{\partial Y_i}{\partial t} + \dot{m} \frac{\partial Y_i}{\partial x} - \frac{\partial F_i}{\partial x} - \dot{\omega} a &= 0, \quad i = 1, \dots, N_s, \\ \rho a \frac{\partial h}{\partial t} + \dot{m} \frac{\partial h}{\partial x} - \frac{\partial H}{\partial x} - \frac{\partial}{\partial x} \left(\sum_{i=1}^{N_s} h_i F_i \right) &= 0, \\ F_i &= \rho a D_{im} \frac{\partial Y_i}{\partial x}, \quad i = 1, \dots, N_s, \\ H &= \frac{\lambda_m a}{C_p} \frac{\partial h}{\partial x}.\end{aligned}\tag{17}$$

For a computational domain over $0 \leq x \leq L$ the corresponding boundary conditions are

$$Y_i = c_i \quad \text{and} \quad h = c_0 \quad \text{at} \quad x = 0, \quad F_i = 0 \quad \text{and} \quad H = 0 \quad \text{at} \quad x = L,$$

where c_i and c_0 are the prescribed constants. Note that since the governing equations are first-order, only Dirichlet boundary conditions are considered.

To proceed, the equations are cast into the vector form

$$\mathbf{A}'_0 \frac{\partial \mathbf{q}}{\partial t} + \mathbf{A}'_1 \frac{\partial \mathbf{q}}{\partial x} + \mathbf{S}' = 0,\tag{18}$$

where $\mathbf{q} = (Y_1, Y_2, \dots, Y_{N_s}, F_1, F_2, \dots, F_{N_s}, h, H)^T$. The time-marching terms are included for numerical convenience and are discretized by the Euler implicit method. The convective term and the source term are linearized in the following fashion:

$$\begin{aligned}\mathbf{q}^{n+1} &= \mathbf{q}^n + \Delta \mathbf{q}, \\ \mathbf{S}'^{n+1} &= \mathbf{S}'^n + \left(\frac{\partial \mathbf{S}'}{\partial \mathbf{q}} \right)^n \Delta \mathbf{q}.\end{aligned}\tag{19}$$

After the manipulation, we obtain a new set of equations in vector form ready for finite element discretization,

$$\mathbf{A}_0^n \Delta \mathbf{q} + \mathbf{A}_1^n \frac{\partial \Delta \mathbf{q}}{\partial x} + \mathbf{A}'_1^n \frac{\partial \mathbf{q}^n}{\partial x} + \mathbf{S}'^n = 0,\tag{20}$$

where superscript n denotes the previous time step. The procedures to construct the least-squares functional and its minimization are standard and we refer the interested readers to Reference 1. An important feature of the LSFEM is that the final global matrix is always symmetric and positive definite. As a result, a simple iterative method such as the Jacobi conjugate gradient method can be used to effectively invert the matrix. Since the problem investigated here is one-dimensional, the results in this paper are obtained by a direct solver.

4. RESULTS AND DISCUSSION

Eberius *et al.*⁴ studied a fuel-rich, low-pressure, H₂/O₂ flame in the laboratory. The reactant ratio in mole fraction was 75 per cent H₂ and 25 per cent O₂. The inlet velocity was 1.78 m s⁻¹ and the pressure was 1413.2 Pa.

As pointed out by Smooke,⁶ there are two approaches to calculate this flame: (i) the temperature profile can be taken from the experimental data and only the species equations are solved or (ii) the species and energy equations are solved together, namely the coupled calculation. Whenever the flame temperature profile is available, the first approach is a better representation of the experiment, because the heat losses of the flame are taken into account. The coupled calculation, on the other hand, usually grossly overpredicts the flame temperature.

Figure 2 shows the convergence history of the calculation with the prescribed temperature profile. The abscissa is the number of time steps and the ordinate is the convergence history. In this calculation, 100 linear elements are used. As shown here, the numerical convergence of H₂, O₂, H₂O and OH are plotted. The initial species distribution contains only H₂ and O₂. Before the flame is numerically ignited, the initial species profile satisfies the governing equations and the initial convergence indicators of H₂ and O₂ are very small. As a contrast, the indicators of H₂O and OH are relatively large. As time goes on, the chemical kinetics trigger the numerical ignition and the product species are generated. Once the species composition is in the ball park, the calculation converges exponentially to machine accuracy.

At the beginning of the calculation a small Δt is used (e.g. $\Delta t = 10^{-4}$ s) to allow suitable resolution for flame ignition. In the subsequent time steps we increase Δt geometrically to about unity in 30 time steps. A large Δt , e.g. 10^{-2} s, for initial calculation will lead to a converged trivial solution without combustion. In addition, when the ignition is triggered numerically, some of the minor species experience violent changes. Therefore in the initial stage of the calculation it is necessary to set a bound to prevent the species mass fraction becoming negative or greater than unity.

Figure 3 shows the calculated mole fraction of H₂, O₂ and H₂O, in which the squares are Eberius *et al.*'s experimental data for H₂O. The abscissa is the streamwise distance in metres and the ordinate is the mole concentrations of species. Since it is a fuel-rich flame, O₂ is consumed completely in the reaction zone. The flame spreads about 2 cm owing to the low pressure. The predicted water vapour profile compares favourably with Eberius *et al.*'s data. Figures 4 and 5 show the mole fraction profile of OH and H. Again, the prediction compares favourably with the experimental data at the flame front and in the reaction zone. However, the calculation overpredicts the OH concentration in the trailing part of the flame.

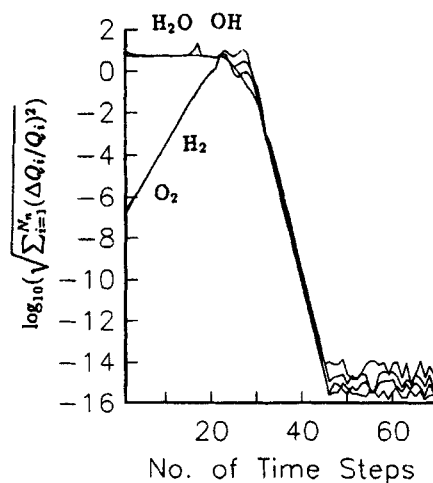


Figure 2. Convergence history of calculation with prescribed temperature profile

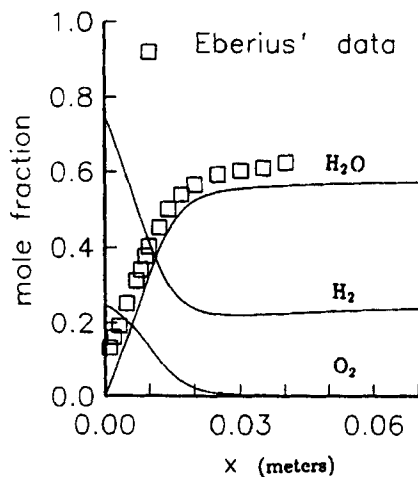


Figure 3. Calculated species distribution of H₂O, H₂ and O₂ with prescribed temperature profile

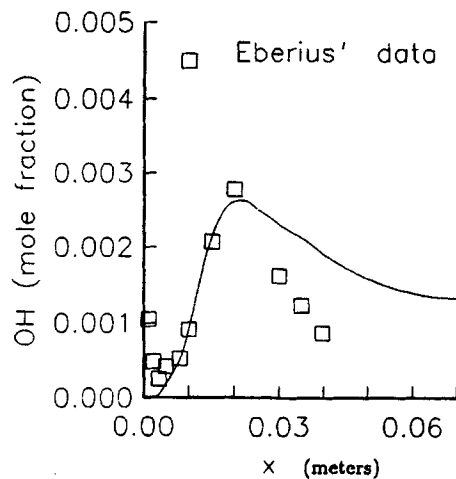


Figure 4. Calculated species distribution of OH with prescribed temperature profile

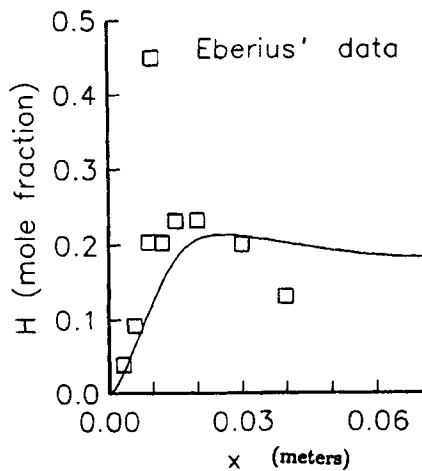


Figure 5. Calculated species distribution of H with prescribed temperature profile

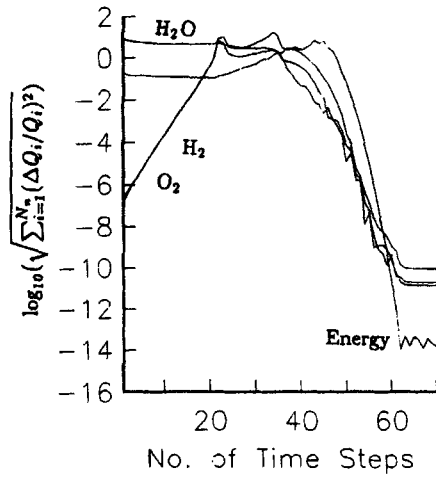


Figure 6. Convergence history of coupled calculation

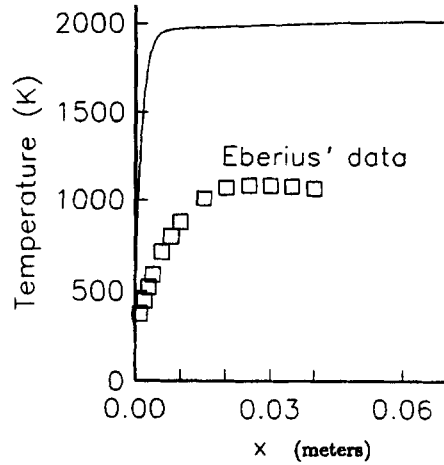


Figure 7. Temperature profile of coupled calculation as compared with Eberius *et al.*'s data

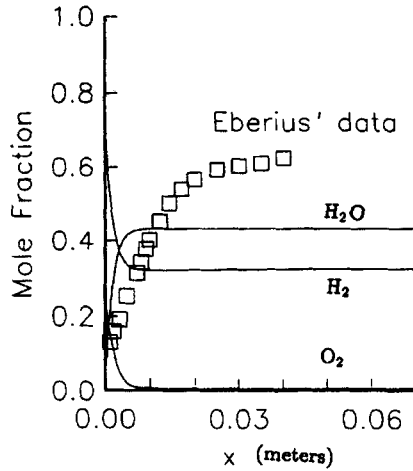


Figure 8. Species distribution of H_2O , H_2 and O_2 of coupled calculation

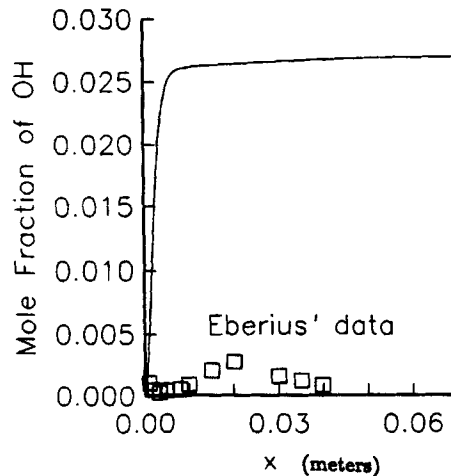


Figure 9. Species distribution of OH of coupled calculation

In Figure 6 the convergence of the energy and H₂, O₂, H₂O and OH species equations are shown for the coupled calculation. The coupled calculation requires an inner iteration for each time step to calculate T and ρ . The convergence criterion of this inner iteration is set to be 10^{-10} , which therefore is also the lower bound of the species convergences. Figure 7 shows the calculated temperature profile as compared with Eberius *et al.*'s data. The simulated flame experiences an abrupt increase in temperature which is much higher than the experimental data. This is because no heat loss effect such as radiation is included in the energy equation. A similar numerical result has been observed by Smooke.⁶ Figures 8 and 9 show the comparisons between the simulated species concentrations and the experimental data. Since the flame temperature is grossly overpredicted, the number of high-energy radicals such as OH is much higher than it should be. Since the mass must be conserved, the existence of the radicals is at the expense of the stable species. Consequently, the water vapour concentration is underpredicted, as shown in Figure 8.

5. CONCLUDING REMARKS

In this paper we report the extension of the LSFEM to simulate a premixed H₂/O₂ flame. A set of quasi-one-dimensional species and energy equations with comprehensive physical property models was solved. Two approaches were taken: first, we solved the species equations with prescribed temperature profile taken from Eberius *et al.*'s experiment; second, the energy equation was solved with species equations in a fully coupled manner. By prescribing the temperature profile, the predicted flame structure compared favourably with the experimental results. In contrast, the coupled calculation grossly overpredicted the flame temperature and the high-energy radicals. The present study shows that the LSFEM is a viable tool for simulating the complex physics of reactive flows.

REFERENCES

1. B. N. Jiang and L. A. Povinelli, 'Least-squares finite element method for fluid dynamics', *Comput. Methods Appl. Mech. Eng.*, **81**, 13-37 (1990).
2. S. T. Yu, B. N. Jiang, N. S. Liu and J. Wu, 'The least-squares finite element method for low-Mach-number compressible viscous flows', *Int. j. numer. methods fluids*, **38**, 3591-3610 (1995).

3. S. T. Yu, B. N. Jiang, J. Wu and N. S. Liu, 'A div-curl-grad formulation for compressible buoyant flows solved by the least-squares finite element method', *Comput. Methods Appl. Mech. Eng.*, in press.
4. K. H. Eberius, K. Hoyerann and H. G. G. Wangner, 'Experimental and mathematical study of a hydrogen-oxygen flame', *Proc. 13th Symp. (Int.) on Combustion*, Combustion Institute, Pittsburgh, PA, 1971, pp. 713-721.
5. J. O. Hirschfelder, C. F. Curtiss and D. F. Campbell, 'The theory of flames and detonations', *J. Chem. Phys.*, **17**, 1076 (1949).
6. M. D. Smooke, 'Solution of burner-stabilized premixed laminar flames by boundary value methods', *J. Comput. Phys.*, **48**, 72-105 (1982).
7. F. A. Williams, *Combustion Theory*, Benjamin/Cummings, New York, 1985.
8. S. Gordon and B. J. McBride, 'Computer program for the calculation of complex equilibrium compositions, rocket performance, incidence and reflected shocks, and Chapman-Jouguet detonations', *NASA SP-273 Interim Revision*, 1976.
9. S. Gordon, B. J. McBride and F. J. Zeleznik, 'Computer program for calculation of complex chemical equilibrium compositions and applications supplement I—transport properties', *NASA TM-86885*, 1984.
10. R. C. Reid, J. M. Prausnitz and B. E. Poling, *The Properties of Gases and Liquids*, McGraw-Hill, New York, 1988.